THE JOURNAL OF BIOLOGICAL CHEMISTRY
Vol. 279, No. 35, Issue of August 27, pp. 36299–36308, 2004

Printed in U.S.A.

Evolution of Vitamin B_2 Biosynthesis

STRUCTURAL AND FUNCTIONAL SIMILARITY BETWEEN PYRIMIDINE DEAMINASES OF EUBACTERIAL AND PLANT ORIGIN*

Received for publication, April 21, 2004, and in revised form, June 16, 2004
Published, JBC Papers in Press, June 18, 2004, DOI 10.1074/jbc.M404406200

Markus Fischer‡, Werner Römisch, Sabine Saller, Boris Illarionov, Gerald Richter, Felix Rohdich, Wolfgang Eisenreich, and Adelbert Bacher

From the Lehrstuhl für Organische Chemie und Biochemie, Technische Universität München, Lichtenbergstrasse 4, Garching D-85747, Germany

The *Arabidopsis thaliana* open reading frame At4g20960 predicts a protein whose N-terminal part is similar to the eubacterial 2,5-diamino-6-ribosylamino-4(3*H*)-pyrimidinone 5′-phosphate deaminase domain. A synthetic open reading frame specifying a pseudomature form of the plant enzyme directed the synthesis of a recombinant protein which was purified to apparent homogeneity and was shown by NMR spectroscopy to convert 2,5-diamino-6-ribosylamino-4(3*H*)-pyrimidinone 5′-phosphate into 5-amino-6-ribosylamino-2,4(1*H*,3*H*)-pyrimidinedione 5′-phosphate at a rate of 0.9 μmol mg^{-1} min^{-1}. The substrate and product of the enzyme are both subject to spontaneous anomerization of the ribosyl side chain as shown by ^{13}C NMR spectroscopy. The protein contains 1 eq of Zn^{2+}/subunit. The deaminase activity could be assigned to the N-terminal section of the plant protein. The deaminase domains of plants and eubacteria share a high degree of similarity, in contrast to deaminases from fungi. These data show that the riboflavin biosynthesis in plants proceeds by the same reaction steps as in eubacteria, whereas fungi use a different pathway.

Flavocoenzymes derived from riboflavin (vitamin B_2; compound **6**, Fig. 1) serve as essential redox cofactors in all cells and have also been shown to be involved in a variety of nonredox processes such as light sensing (1, 2), photorepair of DNA (3), circadian time keeping, and bioluminescence (4–7). Whereas plants and many microorganisms obtain riboflavin by biosynthesis, animals depend on nutritional sources.

The biosynthesis of riboflavin has been studied in some detail in eubacteria and fungi (for review, see Refs. 8–11). Briefly, the first committed step is catalyzed by GTP cyclohydrolase II and involves the hydrolytic release of formate and pyrophosphate from GTP (8–10). The product, 2,5-diamino-6-ribosylamino-4(3*H*)-pyrimidinone 5′-phosphate (**1**), is converted to 5-amino-6-ribitylamino-2,4(1*H*,3*H*)-pyrimidinedione 5′-phosphate (**4**) by deamination of the ring (Fig. 1, *A* and *D*) and reduction of the side chain (Fig. 1, *B* and *C*) (11, 12). In fungi and in eubacteria, these steps have been shown to proceed in the opposite order (Fig. 1).

The intermediate **4**, which is common to the bacterial and fungal pathway, is dephosphorylated by an unknown process affording 5-amino-6-ribitylamino-2,4(1*H*,3*H*)-pyrimidinedione which is condensed with 3,4-dihydroxy-2-butanone 4-phosphate biosynthesized from ribulose 5-phosphate (13–27). The resulting 6,7-dimethyl-8-ribityllumazine (**5**) undergoes a mechanistically unusual dismutation affording riboflavin (**6**) and the dephosphorylated biosynthetic intermediate **4** (19, 28–32).

The biosynthesis of riboflavin in plants has been studied in some detail. A gene specifying a bifunctional GTP cyclohydrolase II/dihydroxybutanone phosphate synthase was cloned from tomato (33, 34). 6,7-Dimethyl-8-ribityllumazine synthase was cloned from spinach, and its structure has been determined by x-ray crystallography (35). Riboflavin synthase was partially purified from spinach (36), and a riboflavin synthase gene was later cloned from *Arabidopsis thaliana* (37).

The conversion of the GTP cyclohydrolase II product **1** into the substrate of lumazine synthase, 5-amino-6-ribitylamino-2,4(1*H*,3*H*)-pyrimidinedione, has not been studied in plants to the best of our knowledge. In this paper, we show that a protein specified by the hypothetical gene At4g20960 of *A. thaliana* catalyzes the deamination of 2,5-diamino-6-ribosylamino-4(3*H*)-pyrimidinone 5′-phosphate (**1**). Thus, riboflavin biosynthesis in plants proceeds by the same reaction steps as in eubacteria, whereas fungi use a different pathway.

EXPERIMENTAL PROCEDURES

Materials—The preparation of [2,1′,2′,3′,4′,5′-$^{13}C_6$]GTP will be described elsewhere. Restriction enzymes were obtained from New England Biolabs and Amersham Biosciences. T4 DNA ligase and reverse transcriptase (Superscript II) were from Invitrogen. Oligonucleotides were custom synthesized by MWG Biotech (Ebersberg, Germany) and by Interactiva (Ulm, Germany). Vent DNA polymerase was purchased from New England Biolabs. A plasmid minipreparation kit from PEQLab (Erlangen, Germany) was used for plasmid DNA isolation and purification. DNA fragments and PCR amplificates were purified with a gel extraction kit or Cycle Pure Kit from PEQLab. Casein hydrolysate and yeast extract were from Invitrogen, and isopropyl β-D-thiogalactopyranoside was from Biomol (Hamburg, Germany). Thrombin was from Sigma. The isolation of recombinant *Escherichia coli* GTP cyclohydrolase II has been described previously (12).

Microorganisms—Bacterial strains and plasmids used in this study are summarized in Table I.

Restriction Enzyme Digestion of DNA—DNA was digested at 37 °C with restriction enzymes in reaction buffers specified by the supplier. The treated DNA was analyzed by horizontal electrophoresis in 0.8–3% agarose gels.

Estimation of Protein Concentration—Protein concentration was estimated by a dye binding assay (38) or photometrically (ϵ_{280nm} for recombinant *A. thaliana* deaminase, 10,600 M^{-1} cm^{-1}).

Transformation of Bacterial Cells—Ligation mixtures were trans-

* This work was supported by grants from the Deutsche Forschungsgemeinschaft, the Fonds der Chemischen Industrie, and the Hans Fischer Gesellschaft. The costs of publication of this article were defrayed in part by the payment of page charges. This article must therefore be hereby marked "*advertisement*" in accordance with 18 U.S.C. Section 1734 solely to indicate this fact.

The nucleotide sequence(s) reported in this paper has been submitted to the GenBank™/EBI Data Bank with accession number(s) AY456384.

‡ To whom correspondence should be addressed. Tel.: 49-89-289-13336; Fax: 49-89-289-13363; E-mail: markus.fischer@ch.tum.de.

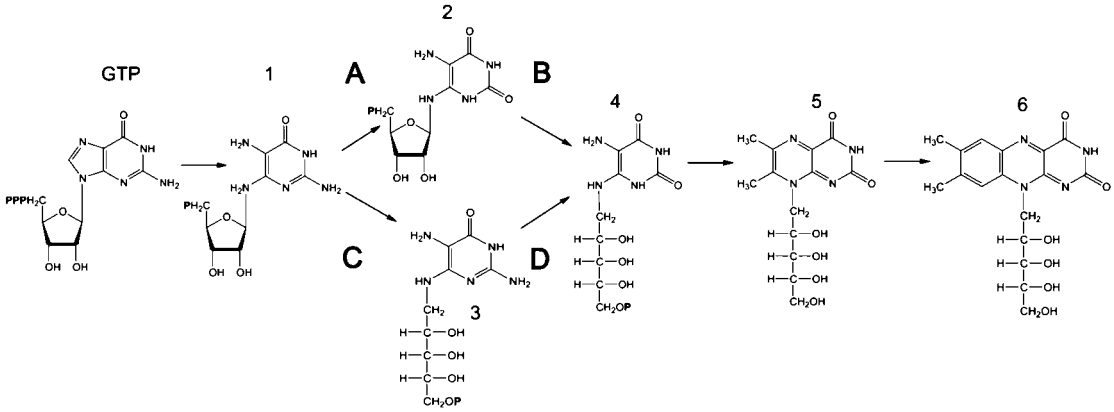

FIG. 1. **Biosynthesis of riboflavin.** Deaminase (*A* and *D*) and reductase (*B* and *C*) reaction steps are shown. The biosynthetic pathway proceeds via *A* and *B* in bacteria and via *C* and *D* in yeasts (11, 52). **1**, 2,5-diamino-6-ribosylamino-4(3*H*)-pyrimidinone 5′-phosphate; **2**, 5-amino-6-ribosylamino-2,4(1*H*,3*H*)-pyrimidinedione 5′-phosphate; **3**, 2,5-diamino-6-ribitylamino-4(3*H*)-pyrimidinone 5′-phosphate; **4**, 5-amino-6-ribitylamino-2,4(1*H*,3*H*)-pyrimidinedione 5′-phosphate; **5**, 6,7-dimethyl-8-ribityllumazine; **6**, riboflavin.

TABLE I
Bacterial strains and plasmids used in this work

Strain or plasmid	Relevant characteristics	Source
E. coli strains		
XL1-blue	recA1 endA1 gyrA96 thi^{-1} hsdR17 supE44 relA1 lac [F9proAB lacI^q ZDM15 Tn10 (Tet^r)]	(39)
M15[pRep4]	lac ara gal mtl recA$^+$ uvr$^+$ (pRep4; lacI Kan^r)	(61)
RR28 rib1	F$^-$ thi pro lac gal ara mtl xyl supE44 endA hsd (r$^-$ m$^-$) pheS recA ribD	(8)
Plasmids		
PNCO113	Plasmid cloning vector, Ap^R	(40)
PACYC184	Plasmid cloning vector, Cm^R	NEB[a]
PNCO-G-Red	Plasmid carrying the gene coding for the reductase domain of *B. subtilis*, based on pNCO113	(11)
PNCO-MalE	pNCO113 containing the *malE* gene of *E. coli*	(41)
PNCO-ATR2-wt	Plasmid carrying the wild type *A. thaliana* deaminase gene, based on pNCO113	This study
PACYC-BSRED	Plasmid carrying the reductase domain of *B. subtilis*, based on plasmid pACYC184	This study
PNCO-ATRib2-syn	pNCO113 carrying a synthetic gene coding for the *A. thaliana* deaminase	This study
PNCO-MalE-TB-ATR2-syn	Plasmid coding coding for a fusion protein consisting of MBP of *E. coli* and the deaminase of *A. thaliana*, based on pNCO-MalE	This study
PNCO-MalE-TB-ATR2–184	Plasmid coding for a fusion protein consisting of MBP of *E. coli* and a deaminase subdomain of *A. thaliana* (amino acids 64–184), based on pNCO-MalE-TB-ATR2-syn	This study
PNCO-MalE-TB-ATR2–250	Plasmid coding for a fusion protein consisting of MBP of *E. coli* and a deaminase subdomain of *A. thaliana* (amino acids 64–250), based on pNCO-MalE-TB-ATR2-syn	This study

[a]New England Biolabs.

formed into *E. coli* XL1-Blue cells (39). Transformants were selected on LB solid medium supplemented with 150 mg/liter ampicillin. The plasmids were reisolated and analyzed by restriction analysis and by DNA sequencing. Sequenced pNCO-type expression plasmids were then transformed into *E. coli* M15 [pREP4] cells (40) carrying the pREP4 repressor plasmid for the overexpression of *lac* repressor protein. 15 mg liter^{-1} kanamycin and 170 mg liter^{-1} ampicillin were added to secure the maintenance of both plasmids in the host strain.

Preparation of cDNA—A 20-μl reaction mixture containing 50 mM Tris-HCl, pH 8.3, 75 mM KCl, 3 mM $MgCl_2$, 10 mM dithiothreitol, 0.5 mM dNTPs, 0.5 μg of oligo$(dT)_{15}$, 2 μg of *A. thaliana* total RNA from leaves, and 200 units of reverse transcriptase was incubated at 37 °C for 15 min and subsequently at 48 °C for 30 min. The mixture was heated at 95 °C for 5 min.

cDNA Cloning—A segment of the hypothetical open reading frame (accession no. At4g20960) was amplified from *A. thaliana* cDNA using the oligonucleotides DN1 and DC1 (Table II) as primers whereby the first 189 bp coding for a putative targeting sequence (63 amino acids) were removed. The amplificate served as template in a second PCR round using the oligonucleotides DN2 and DC2 as primers. A 1.3-kb DNA segment was purified by agarose gel electrophoresis, digested with the restriction endonucleases BamHI and PstI, and ligated into the pNCO113 vector, which had been treated with the same enzymes yielding the plasmid designated pNCO-ATR2-wt.

Gene Synthesis—The protein sequence coded by the pseudomatured open reading frame At4g20960 starting at methionine 64 (without targeting sequence) was retranslated into DNA sequence optimized for the expression in *E. coli* and divided into two segments (part A, bp 1–567; part B, bp 595–1125). Both segments were synthesized by a series of consecutive PCR amplifications and were then ligated. For both segments, synthetic starter DNA fragments (~100 bp) were prepared by PCR with the overlapping oligonucleotides AT-R2–1a and AT-R2–2a (segment A) and AT-R2–1b and AT-R2–2b (Fig. 2, segment B). In a sequence of seven PCR amplifications (segment A), respectively, six PCR amplifications (segment B), the oligonucleotides listed in Table II were used pairwise, starting with AT-R2–3a and AT-R2–4a (segment A) and AT-R2–3b and AT-R2–4b (segment B), for the elongation of each prior amplificate. The final PCR product corresponding to segment A (609 bp) was digested with the restriction endonucleases EcoRI and PstI. The final PCR product corresponding to segment B (552 bp) was digested with PstI and HindIII. Both segments were combined and ligated into the plasmid pNCO113 (18, 38), which had been treated with the restriction enzymes EcoRI and HindIII, yielding the plasmid designated pNCO-ATR2-syn.

Construction of a Plasmid Expressing the Plant Deaminase Fused to the C Terminus of Maltose-binding Protein of E. coli—The synthetic gene coding for the plant deaminase was amplified by PCR using the oligonucleotides ATR2-NotI-Vo and ATR2-HindIII-Hi as primers (Table II) and the plasmid vector pNCO-ATR2-syn as template. The resulting 1119-bp fragment was purified and digested with NotI and HindIII and was then ligated into the plasmid pNCO-MalE (41), which had been treated with the same restriction enzymes yielding the plasmid designated pNCO-MalE-TB-ATR2-syn (Fig. 3).

Construction of Plasmids Expressing Subdomains of the Putative Deaminase of A. thaliana—The expression plasmid pNCO-MalE-TB-ATR2-syn was cleaved with the restriction endonucleases BamHI and HindIII, and a synthetic double-stranded oligonucleotide designated as ATR2–184 was ligated into the vector yielding the plasmid pNCO-MalE-TB-ATR2–184. To generate a further construct the plasmid pNCO-MalE-TB-ATR2-syn was digested with the restriction endonucle-

TABLE II
Oligonucleotides used for construction of expression plasmids

Designation	Sequence (5′ to 3′)
DN1	gtgaagaacaagattcaatagtgat
DC1	gacttgtattcattcatacatgaaaacag
DN2	ga*ggatcc*atgcagatctcatgtctcccaatttggatt
DC2	ga*ctgcag*tcaaaaatagccctctagcaaaacgcttccac
AT-R2–1a	gctactgcatatgtttcccttgaaccatgtaatcattacggccgtacgcctccatgtactgaagcattg
AT-R2–2a	ccaccataccaataacaacacgacgcaccttagctttgatcaatgcttcagtacatggaggcgtacggcc
AT-R2–3a	catgctgaggtgtttgctcttcgcgatgctggtgaactcgctgagaatgctactgcatatgtttcccttgaac
AT-R2–4a	ctttcagacgactaatacccgaagaaaaaacaattggatttggatccaccataccaataacaacacgacg
AT-R2–5a	ggtgacattgttggccaaggtttccatccaaaagctggtcagcctcatgctgaggtgtttgctcttcgc
AT-R2–6a	gcataactcttcttcaacggacacagtaacatcgataccagcatctttcagacgactaatacccgaag
AT-R2–7a	ggttgtacatctcctaatcccatggtaggttgtgtcattgtcaaagatggtgacattgttggccaaggtttc
AT-R2–8a	accggttaacatacgatggatgaaaccctcattcattttcttgcataactcttcttcaacggacac
AT-R2–9a	gattcgttttatatgcgtaagtgtgtggagctcgcaaaacgtgcaattggttgtacatctcctaatcccatg
AT-R2–10a	gacagacatagaataacggagggcgagaaaaggcttaccggttaacatacgatggatgaaacc
AT-R2–11a	atgcgtcgtgaggaagatgttgaagtcgatgattcgttttatatgcgtaagtgtg
AT-R2–12a	atccgaagcaccttgaccaatcttgtcaagcaaacaaccattgacagacatagaataacggagggc
AT-R2–13a	ataata*gaattc*attaaagaggagaaattaactatgcgtcgtgaggaagatgttgaag
AT-R2–14a	tattattat*ctgcag*aagtttcgaatagtaaccaccactatccgaagcaccttgaccaatcttg
AT-R2–1b	ctagttccggtgtcgaaaccgtagtattggaaaagatcaacttggattccattttggattattgttacaac
AT-R2–2b	gacgttaccgcggagatcaagcaagacactgcaaagaccacggttgtaacaataatccaaaatggaatccaag
AT-R2–3b	gtagttttcaccgcaaaggaatcggttgcagaatccggtatctctagttccggtgtcgaaaccgtag
AT-R2–4b	gcaagagtttctgctcaaaaccatcacgcagaagaacttcaagatctttgacgttaccgcggagatcaagcaag
AT-R2–5b	catatccttgcttcttcccacactgtggaagagtcgggcccaaaagttgtagttttcaccgcaaaggaatcg
AT-R2–6b	catcttttgtcgaccattcaggcaggacctcgataattactttctgcaagagtttctgctcaaaaccatc
AT-R2–7b	tcgatccaacctattcagatcatcgtagctagcaatgcgcaacagtctcatatccttgcttcttcccacactg
AT-R2–8b	cacgtgctttgattccagccatttcatcgacgcgatctgacgctcatcttttgtcgaccattcaggcag
AT-R2–9b	tccgatgaactctcgagcatttcttcacaagaagctattaacgtttcgatccaacctattcagatcatc
AT-R2–10b	caagcaaaaccgaaccaccaagttgcttagactgcaaatctttcacgtgctttgattccagccatttc
AT-R2–11b	ataataata*ctgcag*gaatatgatgcgattatccttttcttcctcgctttccgatgaactctcgagcatttc
AT-R2–12b	tattattat*aagctt*aaaaatagccctcaagcaaaaccgaaccaccaagttg
ATR2–184-Fw	gatccaaatccaattgtttttttcttcgggtattagttaaactagta
ATR2–184-Rv	agcttactagtttaactaatacccgaagaaaaaacaattggatttg
ATR2–250-Fw	cgaaactttaaggtaccgtttcccttgaattactta
ATR2–250-Rv	agcttaagtaattcaagggaaacggtaccttaaagttt
ATR2-NotI-Vo	ataataata*gcggccgc*ttcttctggtctggtgccccgcggtcgtcgtgaggaagatgttgaagtc
ATR2-HindIII-Hi	tattattat*aagctt*aaaaatagccctcaagcaaaacc

ases BstBI and HindIII, and a synthetic double-stranded oligonucleotide designated as ATR2–250 was ligated with the vector yielding the plasmid pNCO-MalE-TB-ATR2-250 (Fig. 3).

Construction of a Plasmid Expressing the Reductase Domain of Bacillus subtilis—The plasmid pNCO-G-Red (11) (*ribG* fragment amino acids 113–361) was digested with the restriction enzymes XhoI and BamHI, and the fragment was isolated and ligated into a pACYC184 vector (GenBank X06403), which has been digested with the restriction enzymes SalI and BamHI. The resulting plasmid pACYC-BSRED carries the reductase domain of *B. subtilis* under control of the T5 promotor and the *lac* operator in a low copy vector, which is compatible with pNCO113 expression plasmids.

Complementation Analysis of ribD Mutation in E. coli—The expression plasmids pACYC-BSRED in combination with pNCO-ATR2-wt were transformed *E. coli* Rib1 cells (containing a mutation in the *ribD* gene) (11). 15 mg liter^{-1} chloramphenicol and 170 mg liter^{-1} ampicillin were added to secure the maintenance of both plasmids in the host strain. Aliquots were plated on LB medium containing the appropriate antibiotics. The appearance of transformants was checked after incubation at 30 °C for 24 h.

Purification of Recombinant Proteins—The recombinant *E. coli* strains M15 [pREP4]-pNCO-MalE-TB-ATR2-syn, pNCO-MalE-TB-ATR2–184, and pNCO-MalE-TB-ATR2–250 were grown in LB medium containing 15 mg liter^{-1} kanamycin and 170 mg liter^{-1} ampicillin at 22 °C. At an A_{600nm} of 0.7, isopropyl β-D-thiogalactopyranoside was added to a final concentration of 2 mM. After incubation for 18 h, the cells were harvested by centrifugation (Sorvall GS3 rotor, 5,000 rpm, 15 min, 4 °C), washed twice with 0.9% NaCl, and frozen at −20 °C. Frozen cell mass (5 g) was thawed in 30 ml of buffer A containing 20 mM Tris-HCl, pH 7.4, 200 mM NaCl, 2 mM $MgCl_2$, and 1 mM dithiothreitol. The suspension was cooled on ice and was subjected to ultrasonic treatment Branson Sonifier B-12A, Branson SONIC Power Company, Danbury, CT). The suspension was centrifuged (Sorvall SS34 rotor, 15,000 rpm, 15 min, 4 °C). The supernatant was placed on top of an affinity matrix (composite of amylose/agarose beads, New England Biolabs) which had been equilibrated with buffer A. The column was washed with buffer A and then developed with a linear gradient of 0–10 mM maltose in buffer A. Fractions were combined and concentrated by ultrafiltration.

Partial Proteolysis—The combined fractions from the amylose affinity chromatography were supplemented with 2.5 mM $CaCl_2$ and 1 unit of thrombin/mg of protein. The mixture was incubated at room temperature for 16 h, concentrated to a volume of 5 ml, and placed on a column of Superdex 75 26/60 (Amersham Biosciences) which was then developed with buffer B containing 50 mM Tris-HCl, pH 7.4, 100 mM KCl, and 1 mM $MgCl_2$). Fractions were combined and concentrated by ultrafiltration.

Native Molecular Mass—Native molecular mass was estimated using a Pharmacia FPLC system equipped with a Superose 6 HR (30 × 1.6 cm) column (Amersham Biosciences). The elution buffer contained 50 mM Tris-HCl, pH 7.4, 100 mM KCl, and 1 mM $MgCl_2$. The column was calibrated using the following standard proteins: RNase A (13.7 kDa), chymotrypsinogen A (25.0 kDa), ovalbumin (43.0 kDa), bovine serum albumin (67.0 kDa), aldolase (158 kDa), catalase (232 kDa), and apoferritin (440 kDa).

DNA Sequencing—Sequencing was performed by the Sanger dideoxy chain termination method (42). Plasmid DNA was isolated from 5-ml cultures of XL1-Blue strains grown overnight in LB medium containing 170 mg/liter ampicillin using a plasmid minipreparation kit from PEQLab. Custom sequencing was performed by MWG Biotech.

SDS-PAGE—SDS-PAGE was performed by procedures published previously (43).

Protein Sequencing—Sequence determination was performed by the automated Edman method using a 471 A protein sequencer (PerkinElmer Life Sciences).

Atomic Absorption Spectroscopy—Purified protein (4.8 mg/ml) was dialyzed against 50 mM Tris-HCl, pH 8.0. The solution was analyzed in a graphite furnace atomic absorption spectrograph Varian spectrAA-100 (Varian Deutschland GmbH, Darmstadt, Germany). The dialysis buffer was used as reference, and 0.1 M zinc sulfate was used as standard.

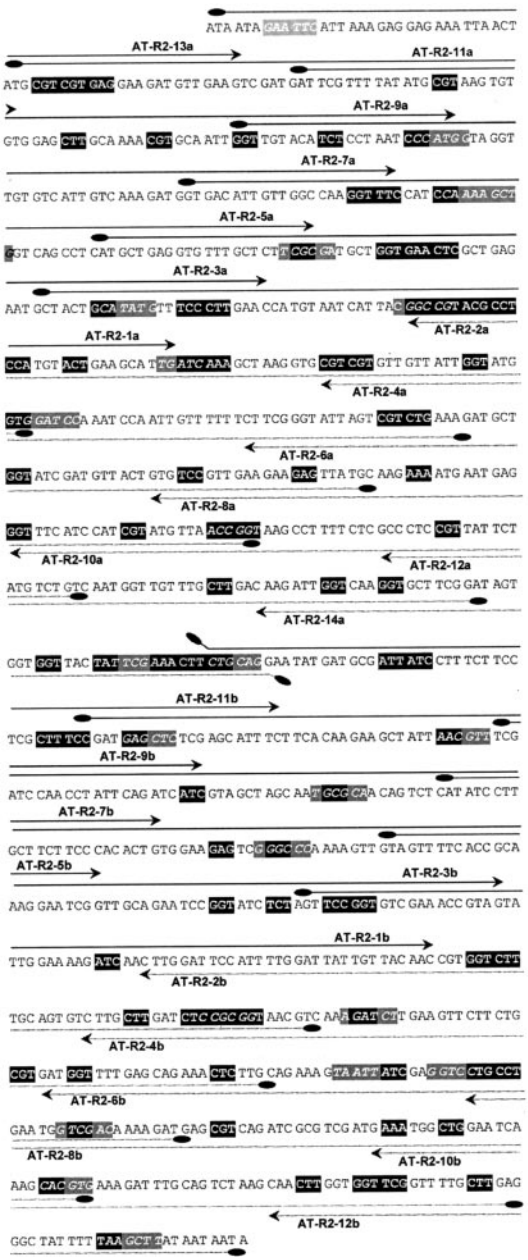

FIG. 2. **Strategy for preparation of the synthetic gene coding for *A. thaliana* 2,5-diamino-6-ribosylamino-4(3*H*)-pyrimidinone 5′-phosphate deaminase with improved codon usage for the expression in *E. coli*.** Changed codons are marked by *black boxes*. New recognition sites for singular restriction endonucleases are drawn in *italics*. *Gray boxes* indicate sequence parts that contribute to the restriction site but are also present in the wild type gene.

Electrospray Mass Spectroscopy—Experiments were performed as described elsewhere (44).

NMR Spectroscopy—Samples were dissolved in 0.5 ml of 50 mM Tris, pH 7.8, containing 10 mM $MgCl_2$, 5 mM dithiothreitol, and 10% D_2O. ^1H and ^{13}C spectra were acquired with a DRX 500 spectrometer from Bruker Instruments, Karlsruhe, Germany, at transmitter frequencies of 500.13 and 125.76 MHz, respectively. The standard temperature was 17 °C, and 37 °C for kinetic measurements. Two-dimensional HMQC,[1] TOCSY, and INADEQUATE spectra were measured using standard Bruker software (XWINNMR 3.0). The mixing time was 60 ms in the ^{13}C TOCSY experiment. Composite pulse decoupling was used for ^{13}C NMR measurements. 3-(Trimethylsilyl)-1-propanesulfonate served as an external standard for ^1H and ^{13}C NMR measurements.

Sequence Alignment and Phylogenetic Analysis—Amino acid sequences of *E. coli* (accession no. P25539) and *B. subtilis* (accession no. P17618) riboflavin type deaminase/reductase genes were used to query nonredundant NCBI (www.ncbi.nlm.nih.gov/) and plant cDNA/expressed sequence tag data bases (www.plantgdb.org/cgi-bin/PlantGDBblast) using the BLAST algorithm (45). Protein sequences were aligned using ClustalW (clustalw.genome.ad.jp/) and edited by hand to remove positions with gaps. Phylogenetic analysis was carried out based on an alignment using 54 translated eubacterial and 9 plant genes and the program package TreeTop (www.genebee.msu.su/services/phtree_full.html). The length of the alignment has been adapted to the deaminase domain of *A. thaliana* starting from position 64 to position 250, which can fold independently, yielding enzymatically active protein.

RESULTS

The product of a putative open reading frame of *A. thaliana* (accession no. At4g20960 (46)) shows similarity to the *ribG* gene specifying the deaminase domain of the bifunctional pyrimidine deaminase/reductase of *B. subtilis* (Fig. 4) (11). A hypothetical plastid targeting sequence of about 63 amino acid residues precedes the plant deaminase domain. Sequence analysis with the software package ChloroP (47, 48) suggested that the gene comprises an N-terminal plastid targeting sequence; this agrees well with the earlier finding that several other enzymes of the riboflavin pathway of plants carry typical plastid targeting sequences (33, 34, 37, 49). The *in silico* analysis with software SignalP suggested a cutting site between the amino acid residues 63 and 64. The mature form should thus begin with the N-terminal sequence MRREEDVEVDDSFY.

Based on these findings, a DNA segment extending from bp 190 to 1280 (deaminase domain without the putative plastid targeting sequence) was amplified from *A. thaliana* cDNA and was cloned into the pNCO113 plasmid vector. The nucleotide sequence of the cloned cDNA segment showed no differences by comparison with the previously published genomic sequence data and confirmed the predicted intron location in the chromosomal gene located on *A. thaliana* chromosome 4 from 11211957 to 11213651 (predicted exon topology, 1–500, 597–895, 973–1695) (46). A recombinant *E. coli* strain harboring the plant gene segment on an expression plasmid under the control of a T5 promoter and *lac* operator produced only small amounts of the predicted protein.

Because the wild type plant gene under study comprises numerous codons that are known to be poorly transcribed in *E. coli*, the yield of expressed recombinant enzyme was very low. To overcome these problems we synthesized a synthetic gene whose sequence was optimized for expression in *E. coli* (Fig. 2). The aim was to produce sufficient amounts of the plant protein required for a detailed functional characterization and, ultimately, crystallization studies. For that purpose, 87 codons were replaced. Moreover, 20 new unique restriction sites were implemented (Fig. 2). The optimized sequence has been deposited in GenBank (accession no. AY456384).

This optimized heterologous system showed a very high expression level. Unfortunately, a strong tendency of the protein to accumulate in inclusion bodies limited the final recovery level. To minimize the aggregation behavior, a fusion protein consisting of the maltose-binding protein of *E. coli* fused to the N terminus of the plant deaminase was constructed. Between both domains a short linker sequence including a thrombin cleavage site was introduced (Fig. 3). A recombinant *E. coli* strain harboring a plasmid with that sequence under the control of a T5 promotor and a *lac* operator produced large amounts of a soluble recombinant protein with an apparent mass of 83 kDa as judged by SDS-PAGE (Fig. 5).

[1] The abbreviations used are: HMQC, heteronuclear multiple quantum coherence; MBP, maltose-binding protein; NOESY, nuclear Overhauser effect spectroscopy; TOCSY, total correlation spectroscopy; INADEQUATE, incredible natural abundance double quantum transfer experiment.

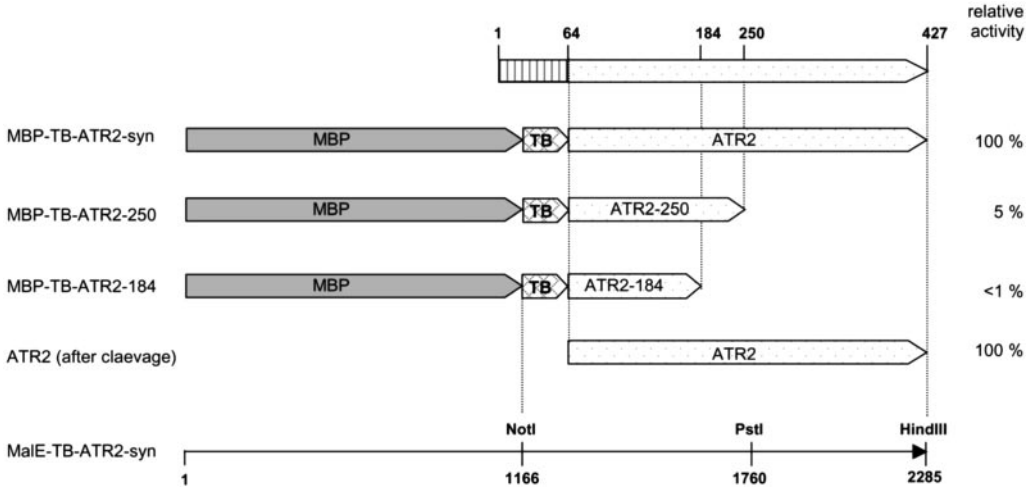

FIG. 3. **Schematic view of plasmid constructs used in this study.** *First line*, sequence corresponding to open reading frame At4g20960; *MBP-TB-ATR2-syn*, synthetic gene coding for the deaminase domain (amino acids 64–427) of *A. thaliana* fused to the C terminus of maltose-binding protein (*MBP*) of *E. coli* via a recognition sequence for thrombin (*TB*); *MBP-TB-ATR2–250*, construct with a C-terminal truncated deaminase domain (amino acids 64–250) of *A. thaliana*; *MBP-TB-ATR2–184*, construct with a C-terminal truncated deaminase domain (amino acids 64–184) of *A. thaliana*; *MalE-TB-ATR2-syn*, genetic map of the coding region of the synthetic construct expressing MBP-TB-ATR2-syn.

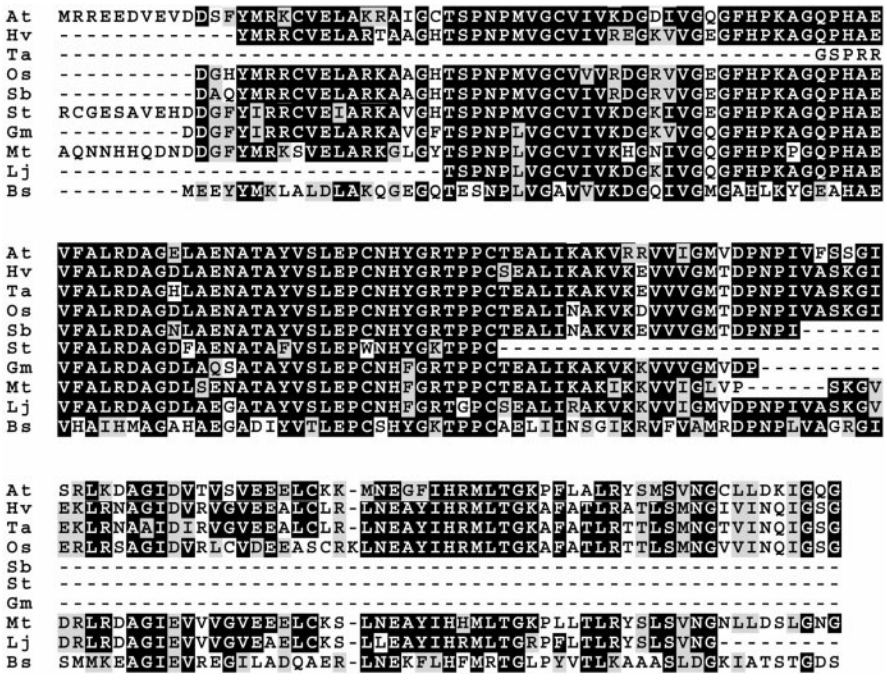

FIG. 4. **Primary structures of deduced plant 2,5-diamino-6-ribosylamino-4(3*H*)-pyrimidinone 5′-phosphate deaminase domains and the deaminase domain of the RibG protein of *B. subtilis*.** *At*, *A. thaliana* (NCBI accession CAB79096.1); *Bs*, *B. subtilis* RibG (NP_390209). The following open reading frames were deduced from nucleotide sequences available at The TIGR Gene Indices Data Base: barley, *Hordeum vulgare* (*Hv*, TC35422); legume, *Medicago truncatula* (*Mt*, TC50740); lotus, *Lotus japonicus* (*Lj*, AV426745); wheat, *Triticum aestivum* (*Ta*, TC62433); soybean, *Glycine max* (*Gm*, TC129327); sorghum, *Sorghum bicolour* (*Sb*, BE600990); rice, *Oryza sativa* (*Os*, AK070281); potato, *Solanum tuberosum* (*St*, TC42758). The length of the alignment has been adapted to the deaminase domain of *A. thaliana* starting from position 64 to position 250, which can fold independently, yielding enzymatically active protein.

The recombinant fusion protein was purified by affinity chromatography on amylose affinity matrix. The maltose binding domain was then cleaved off by thrombin digestion, and the pseudomature plant deaminase domain was isolated in apparently pure form by gel permeation chromatography (Fig. 5). Partial Edman degradation afforded the expected N-terminal sequence GRREEDVEDDSFYM. Mass spectrometry afforded a relative mass of 39.650 Da in good agreement with the calculated mass of 39.655 Da. Whereas the engineered protein is believed to start with Gly because of the introduction of the thrombin cleavage site, the wild type protein carries Met in the corresponding position.

In the pseudomature deaminase domain of *A. thaliana* one zinc ion/subunit was found by atomic absorption spectroscopy.

Earlier, we could show by NMR analysis that the product of GTP cyclohydrolase II forms a mixture of α and β anomers (13). More specifically, the direct reaction product is the β anomer, which can yield the α anomer by spontaneous anomerization The ratio of the α and β anomers at equilibrium has been reported as 1:1.4 on the basis of studies with [1′,2′,3′,4′,5′-$^{13}C_5$]GTP (9).

As an extension of the previous work, we have now prepared [2,1′,2′,3′,4′,5′-$^{13}C_6$]GTP, which afforded [2,1′,2′,3′,4′,5′-$^{13}C_6$]2,5-diamino-6-ribosylamino-4(3*H*)-pyrimidinone 5′-phosphate after treatment with GTP cyclohydrolase II. Notably, in that isotopolog, the position 2 carbon atom of the pyrimidine ring, which is subject to deamination, carries a ^{13}C label. Two ^{13}C signals at 151.2 and 151.6 ppm of slightly different intensity represent the position 2 carbon atoms of the two different anomers of the GTP cyclohydrolase II product. In GTP cyclohydrolase II reaction mixtures, the signal at 151.2 ppm appears more rapidly than the signal at 151.6 ppm, indicating that C-2 of the β-anomer of **1** resonates at 151.2 ppm.

The addition of *A. thaliana* pyrimidine deaminase to the reaction mixture containing [2,1′,2′,3′,4′,5′-$^{13}C_6$]2,5-diamino-6-ribosylamino-4(3*H*)-pyrimidinone 5′-phosphate resulted in the disappearance of the signals at 151.2 and 151.6 ppm (GTP cyclohydrolase II product **1**, Fig. 1) and the appearance of

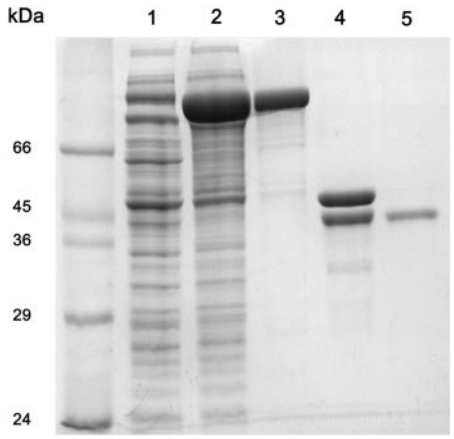

FIG. 5. **SDS-PAGE. 1**, crude extract of *E. coli* M15 [pREP4]-pQE-ATR2-wt; **2**, crude extract of the *E. coli* strain M15 [pREP4]-pNCO-MalE-TB-ATR2-syn; **3**, MBP-deaminase protein derived from *E. coli* strain M15 [pREP4]-pNCO-MalE-TB-ATR2-syn after purification on an amylose column; **4**, MBP-deaminase protein after treatment with thrombin; **5**, deaminase of *A. thaliana* after purification on the Superdex 75 column.

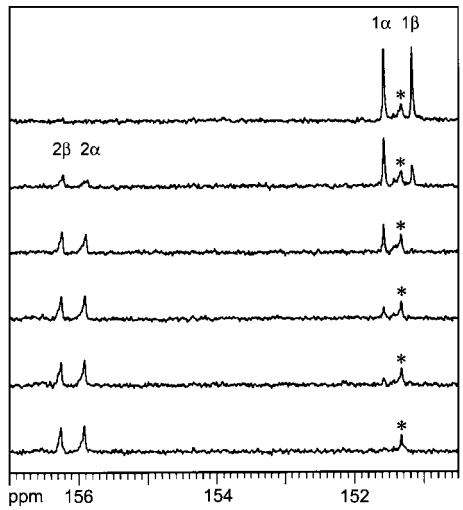

FIG. 6. **Time-resolved ^{13}C NMR signals of the labeled C-2 carbon during the reaction starting from a mixture of 1α and 1β to a mixture of 2α and 2β.** Notably the signal of **1β** disappears first, and the signal of **2β** appears first in comparison to the α anomers.

signals at 156.1 and 155.7 ppm (deaminase product **2**, Figs. 1 and 6). Notably, the signal at 151.2 ppm disappears more rapidly than that at 151.6 ppm, and the signal at 156.1 ppm appears more rapidly compared with that at 155.7 ppm. The signals of the enzyme product at 156.1 and 155.7 ppm appear broader than those of the substrate at 151.2 and 151.6 ppm.

The signals of the *A. thaliana* deaminase product obtained from [2,1′,2′,3′,4′,5′-$^{13}C_6$]**1** are shown in Fig. 7*A*. The complex multiplet patterns arises by $^{13}C^{13}C$ coupling. Notably, the ^{13}C NMR signals observed in the spectrum of a conversion of [2,1′,2′,3′,4′,5′-$^{13}C_6$]**1** with the bifunctional deaminase/reductase from *E. coli* are apparently identical (Fig. 7*B*). This indicates that the *A. thaliana* deaminase product is identical with that obtained from the *E. coli* enzyme, namely 5-amino-6-ribosylamino-2,4(1*H*,3*H*)-pyrimidinedione 5′-phosphate (11). This conclusion is confirmed by a detailed NMR analysis including two-dimensional $^1H^{13}C$ and $^{13}C^{13}C$ correlation experiments (Table III). Two-dimensional INADEQUATE measurements afforded the $^{13}C^{13}C$ connectivities of carbon atoms 1′ with 2′ and of 4′ with 5′ of both anomers (Fig. 8). Two-dimensional $^{13}C^{13}C$ TOCSY spectroscopy confirmed these correlations and afforded additional ^{13}C correlations conducive to the complete assignments of both spin systems (Fig. 9 and Table III). On the basis of kinetic arguments (for details, see above), the C-2 signals at 155.7 and 156.1 ppm can be assigned to the α and β anomers, respectively.

The $^1H^{13}C$ connectivities in the carbon moieties of the glycosides **2α** and **2β** can be assigned on the basis of the $^1H^{13}C$ correlation spectra. The HMQC spectrum (Fig. 10) shows cross-signals for pairs of directly connected $^1H^{13}C$ pairs. The HMQC-TOCSY spectrum identifies pairs of hydrogen atoms on vicinal carbon atoms. The chemical shifts of both respective anomers are summarized in Table III.

The sequence of events following the addition of deaminase to 2,5-diamino-6-ribosylamino-4(3*H*)-pyrimidinone 5′-phosphate produced by the action of GTP cyclohydrolase II product is summarized in Reaction 1.

$$\mathbf{1\alpha} \underset{k_2}{\overset{k_1}{\rightleftharpoons}} \mathbf{1\beta} \xrightarrow{k_3} \mathbf{2\beta} \underset{k_5}{\overset{k_4}{\rightleftharpoons}} \mathbf{2\alpha}$$

REACTION 1

This kinetic network can be described by the following set of rate equations.

$$d([\mathbf{1\alpha}])/dt = -[\mathbf{1\alpha}]\cdot k_1 + [\mathbf{1\beta}]\cdot k_2 \quad \text{(Eq. 1)}$$

$$d([\mathbf{1\beta}])/dt = [\mathbf{1\alpha}]\cdot k_1 - [\mathbf{1\beta}]\cdot k_2 - [\mathbf{1\beta}]\cdot k_3 \quad \text{(Eq. 2)}$$

$$d([\mathbf{2\beta}])/dt = [\mathbf{1\beta}]\cdot k_3 - [\mathbf{2\beta}]\cdot k_4 + [\mathbf{2\alpha}]\cdot k_5 \quad \text{(Eq. 3)}$$

$$d([\mathbf{2\alpha}])/dt = [\mathbf{2\beta}]\cdot k_4 - [\mathbf{2\alpha}]\cdot k_5 \quad \text{(Eq. 4)}$$

The quantitative analysis of the signals in the time-resolved NMR spectra affords the concentrations of all reactants under study. Fitting these data to the set of rate equations yields the data shown in Fig. 11 and Table IV. Notably, the rate constants $k_{1/2}$ and $k_{4/5}$ characterizing the isomerization reactions are all similar, in the range of 0.11–0.20 min^{-1}. The specific activity of the plant deaminase is 0.9 μmol mg^{-1} min^{-1}.

To obtain more evidence on the evolution of the riboflavin biosynthetic pathway of plants, we performed a comprehensive sequence data base search. A BLAST search with the *A. thaliana* deaminase domain studied in this paper as the search motif revealed significant sequence similarity with the N-terminal section of the bifunctional RibD protein of *B. subtilis* and of putative orthologs from a wide variety of eubacteria and from several plant species (Fig. 4).

An initial complementation assay showed that a chromosomal *ribD*$^-$ mutant strain (Rib1) could not be reconstructed by the putative *A. thaliana* gene. More sophisticated complementation analysis showed that the phenotype of the mutant strain could be restored by plasmids directing the synthesis of the plant deaminase in combination with the eubacterial reductase domain. This means that the putative *A. thaliana* protein failed to catalyze the reduction of compound 2 (Fig. 1). In a cross-checking experiment the *A. thaliana* gene was coexpressed with the fungal type (*Saccharomyces cerevisiae*) reductase (*RIB7*) and deaminase (*RIB2*) gene. In both cases no complementation could be observed. This fact is remarkably well in line with the data base and the NMR analysis and means that the second step in the riboflavin pathway of *A. thaliana* is identical to the reaction found in eubacteria.

The N-terminal part of RibD proteins of eubacterial organisms is known to harbor the deaminase domain (11). Based on sequence alignments with functional deaminase domains of *B. subtilis*, C-terminal truncated plant proteins were constructed (Fig. 3). A subdomain consisting of amino acid residue 64–250 of the pseudomature plant enzyme was found to be sufficient for deaminase activity. These data suggest that the putative

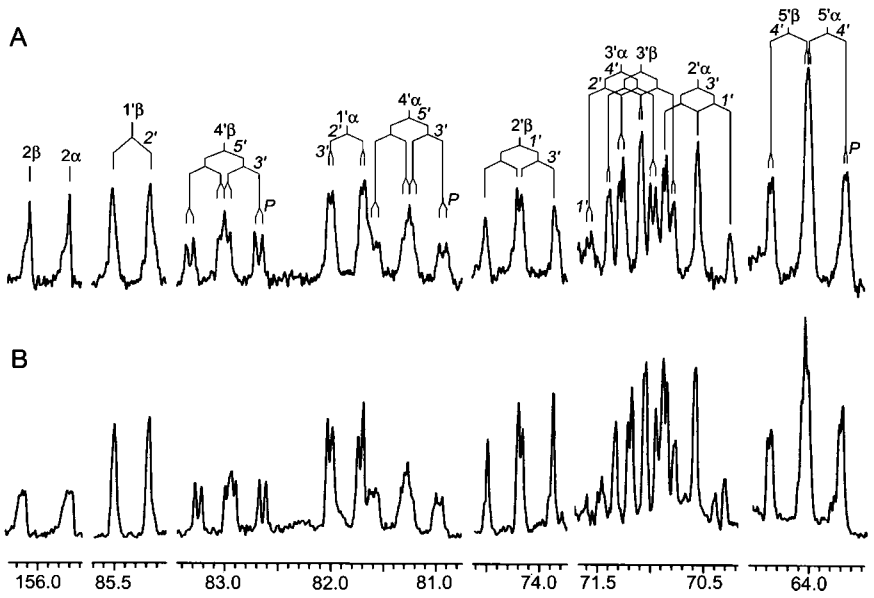

FIG. 7. **^{13}C NMR signals of the product mixture obtained by treatment of [2,1′,2′,3′,4′,5′-$^{13}C_6$]GTP with GTP cyclohydrolase II and deaminase from *A. thaliana* (*A*) or bifunctional deaminase/reductase from *E. coli* (*B*).**

TABLE III
NMR data of [2,1′,2′,3′,4′,5′-$^{13}C_6$]5-amino-6-ribosylamino-2,4(1H,3H)-pyrimidinedione 5′-phosphate

Position	Chemical shift		Coupling constants		Correlation pattern		
	^{1}H	^{13}C	J_{CC}	J_{CP}	INADEQUATE	^{13}C TOCSY	HMQC-TOCSY
	ppm		*Hz*				
Compound 2*α*							
2		155.7					
1′	5.63	81.8	38.5 (2′)		2′	2′,3′,4′,5′	2′,3′
			4.9 (3′)				
2′	4.14	70.5	37.3 (1′,3′)		1′	1′,3′,4′,5′	1′,4′
3′	4.14	71.3	38.3 (2′)			1′,2′,4′,5′	1′,4′
			37.4 (4′)				
			4.9 (1′)				
4′	3.92	81.2	44.1 (5′)	8.2	5′	1′,2′,3′,5′	2′,3′,5′
			35.9 (3′)				
5′	3.68	63.8	43.7 (4′)	3.0	4′	1′,2′,3′,4′	2′,3′,4′
Compound 2*β*							
2		156.1					
1′	5.41	85.3	44.7 (2′)		2′	2′,3′,4′,5′	2′,3′
2′	4.08	74.2	43.9 (1′)		1′	1′,3′,4′,5′	1′
			38.4 (3′)				
3′	4.08	71.1	38.2 (2′,4′)			1′,2′,4′,5′	1′,4′
			2.2 (1′)				
4′	3.91	83.0	44.6 (5′)	8.5	5′	1′,2′,3′,5′	3′,5′
			37.0 (3′)				
5′	3.63	64.2	43.2 (4′)	3.9	4′	1′,2′,3′,4′	4′

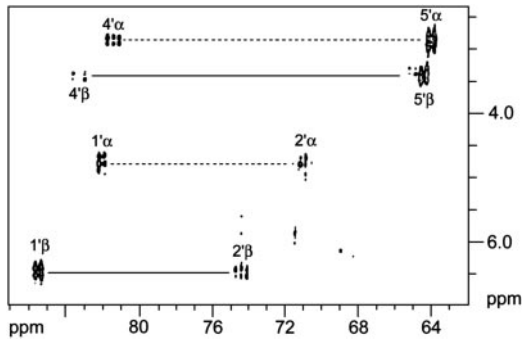

FIG. 8. **Two-dimensional INADEQUATE spectrum of the deaminase products.** The correlated signals of **2*α*** and **2*β*** are connected via *dashed* and *solid lines*, respectively.

open reading frame of *A. thaliana* directs the synthesis of a deaminase subdomain, which can fold independently.

Extended sequence analysis showed homology to a wide variety of eubacterial and plant sequences. The similarity between the cognate protein sequences is illustrated by the dendrogram in Fig. 12. Notably, all plant deaminase sequences form a cluster in the phylogenetic tree. It is also worth noting that Gram-negative bacteria form a subcluster by themselves; the same is true for the group of Gram-positive eubacteria with only a few exceptions. The plant sequences are in close neighborhood to cyanobacteria, plant pathogens, and soil bacteria. Remarkably, 1 of 17 completely sequenced archaebacterial species (*Pyrococcus furiosus*) carries a putative gene with close similarity to the bifunctional RibD protein of *B. subtilis* and does not contain any putative orthologs of the *Methanococcus jannaschii* pyrimidine nucleotide reductase (50) which is believed to catalyze the fungal type reduction of the ribosyl side chain in Archaea. Notably, only one eubacterium (*Buchnera aphidicola*, subsp. Schizaphis graminum) carries separate genes for the deaminase (accession no. Q8K9A4) and the reductase (accession no. Q8K9A3), however, in a sequential order.

Pyrimidine deaminases of the riboflavin pathway show also sequence homology to yeast cytosine deaminase (Fig. 13). The enzyme has been found in prokaryotes and fungi, where it is a member of the pyrimidine salvage pathway. The x-ray structure of yeast cytosine deaminase has been determined in the

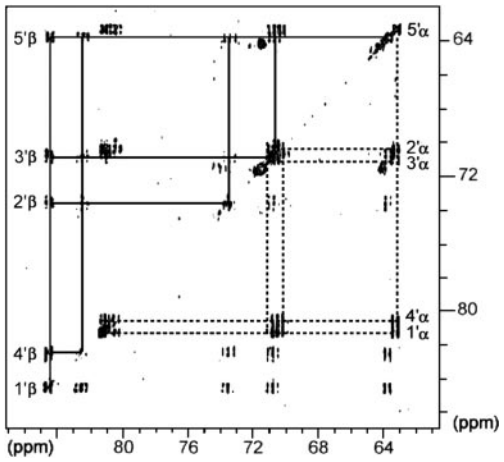

FIG. 9. **Two-dimensional $^{13}C^{13}C$ TOCSY spectrum of the deaminase products.** The correlated signals of the two spin systems of **2*α*** and **2*β*** are connected by *dashed* and *solid lines*, respectively.

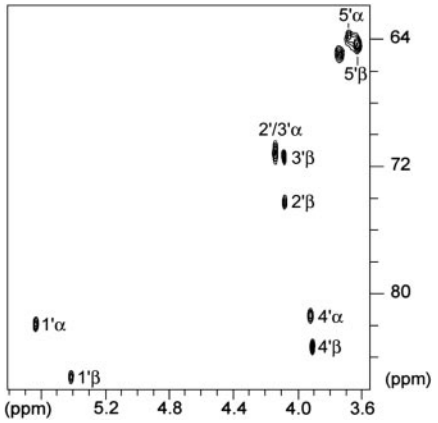

FIG. 10. **Two-dimensional $^1H^{13}C$ correlation spectrum of the product mixture obtained by treatment of [2,1′,2′,3′,4′,5′-$^{13}C_6$]GTP with GTP cyclohydrolase II and deaminase from *A. thaliana*.**

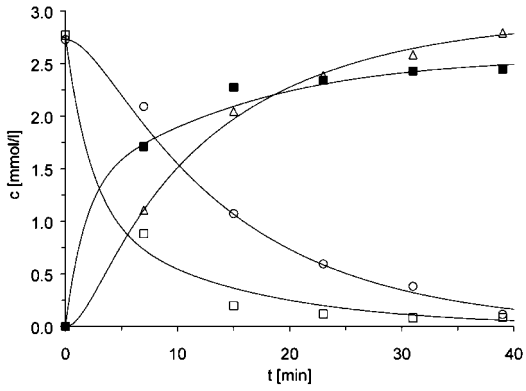

FIG. 11. **Reaction dynamics of deaminase from *A. thaliana*.** The time-resolved concentration was calculated from the integrals of the ^{13}C-labeled C-2 carbon atoms of the reactants **1*α*** (○), **2*β*** (□), **2*α*** (△), and **2*β*** (■) (see Fig. 6).

TABLE IV
Kinetic parameters of pyrimidine deaminase of A. thaliana obtained from ^{13}C NMR spectroscopy

Reaction	Kinetic parameter	Value
1*α* → **1*β***	k_1	0.11 min^{-1}
1*β* → **1*α***	k_2	0.11 min^{-1}
1*β* → **2*β***	k_3	1.34 min^{-1} mg^{-1}
2*β* → **2*α***	k_4	0.20 min^{-1}
2*α* → **2*β***	k_5	0.18 min^{-1}
1(*α*/*β*) → **2(*α*/*β*)**	V_{max}	0.9 μmol min^{-1} mg^{-1}

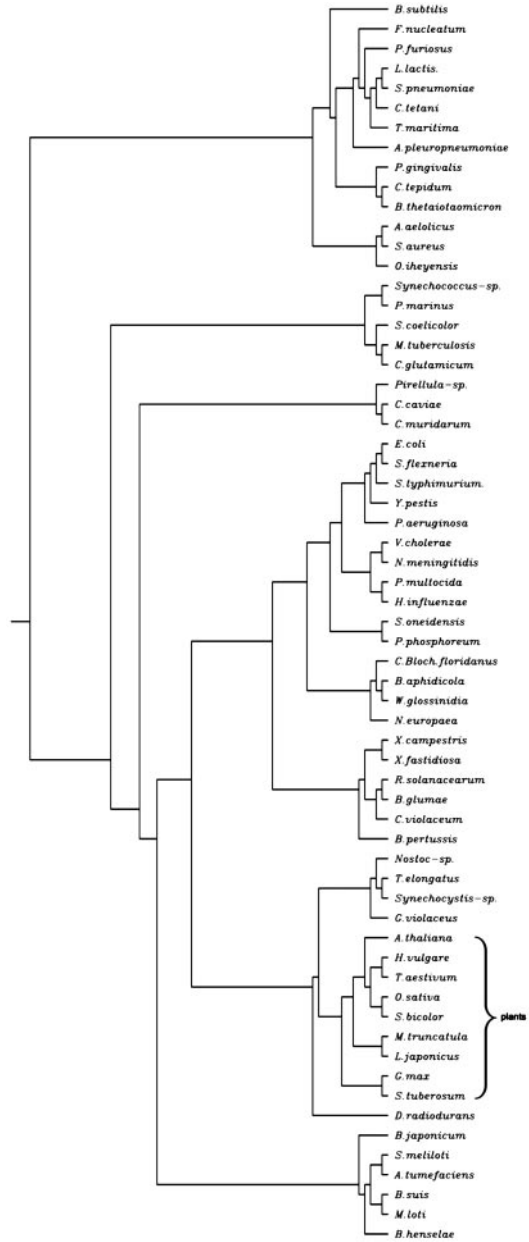

FIG. 12. **Phylogenetic tree of 2,5-diamino-6-ribosylamino-4(3*H*)-pyrimidinone 5′-phosphate deaminase domains.**

presence of an inhibitor at 1.14 Å resolution (51). Each active site contains a single catalytic zinc ion that is coordinated by a histidine, two cysteines, and a single bound water molecule that was found to act as a nucleophile in the deamination reaction. The coordination site for the zinc ion, which is known from the structure of the yeast cytosine deaminase, is strictly conserved over 54 bacterial and 9 plant pyrimidine deaminases of the riboflavin pathway analyzed in this study (Fig. 13). Some of the residues of the active site cavity of the cytosine deaminase are also present and highly conserved in riboflavin type deaminases, *e.g.* residues corresponding to His-62 (His-58 in the pseudomature *A. thaliana* deaminase), Glu-64 (Glu-60), Leu-88 (Leu-80), and Cys-91 (Cys-83). (Fig. 13). In addition, sequence similarity is also found to bacterial cytidine deaminase, *e.g.* of *E. coli* (accession no. P13652).

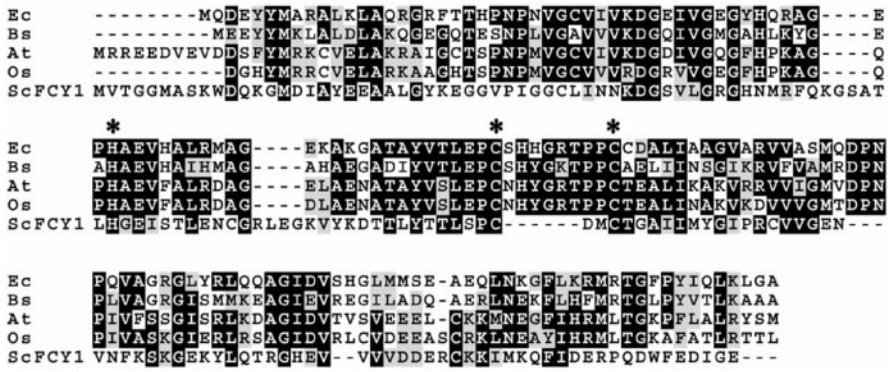

FIG. 13. **Sequence alignment of 2,5-diamino-6-ribosylamino-4(3*H*)-pyrimidinone 5′-phosphate deaminases from eubacteria and plants and cytosine deaminase from *S. cerevisiae*.** *At*, *A. thaliana* (At4g20960); *Bs*, *B. subtilis rib*G (P17618); *Ec*, *E. coli* (Q8FKC3); *Os*, *O. sativa* (AK070281); and *ScFCY1*, and cytosine deaminase of *S. cerevisiae* (Q12178). The highly conserved zinc coordination site of yeast cytosine deaminase is indicated by *asterisks*.

Functional residues involved in zinc coordination or in the fixation of the substrate are present in all three enzymes, the pyrimidine, the cytosine, and the cytidine deaminases. This homology could indicate that deaminases of that group have evolved from a common origin selected to perform a similar reaction on the basis of different substrate molecules.

DISCUSSION

Although the terminal steps in the riboflavin pathway of plants have been studied in considerable detail (33–35, 37), the earlier enzymes of the pathway, most notably the pyrimidine deaminases and pyrimidine reductases, are less well understood. Earlier work had indicated that the product of GTP cyclohydrolase II, 2,5-diamino-6-ribosylamino-4(3*H*)-pyrimidinone 5′-phosphate, is subject to deamination in the eubacteria, *E. coli* and *B. subtilis* (11) but instead undergoes side chain reduction in the yeast, *S. cerevisiae* (52, 53). This sequence of events had been correctly derived from early studies on products produced and excreted by riboflavin-deficient mutants of *S. cerevisiae* (54–57).

Enzymes catalyzing the reduction of the ribose chain of **1** under formation of **3** have been partially purified from the flavogenic ascomycete *Ashbya gossypii* (53) and from *Candida guillermondii* (52). The enzyme catalyzing the reduction of **1** has been cloned from the yeast *C. guillermondii* (58). Genes involved in the riboflavin pathway of *S. cerevisiae* and *A. gossypii* have been claimed in patents (59, 60). Moreover, although reductase and deaminase occur as separate enzymes in *S. cerevisiae* and other fungi, bifunctional proteins with deaminase and reductase activity were found in the eubacteria, *E. coli* and *B. subtilis* (11). The deaminase as well as the reductase domain of the bifunctional enzyme of *B. subtilis* could be expressed separately as functional proteins (11).

The data reported in this paper show that the enzyme of *A. thaliana* deaminates the product of GTP cyclohydrolase II at a rate of 0.9 μmol mg^{-1} min^{-1}. This rate is similar to that of the enzyme of *E. coli* (0.36 μmol mg^{-1} min^{-1}) (15).

The substrate and the product of deaminase are both subject to spontaneous epimerization. The equilibrium constant for each respective pair of anomers has a value close to 1, and the velocities of anomerization for the two anomer pairs are similar. Spontaneous hydrolysis of the *N*-glycosidic bond is slow compared with the epimerization reaction.

It has not been possible, up to now, to determine directly the absolute configuration of these anomers because NOESY spectrometry gave insufficient results. It can be shown, however, on the basis of kinetic arguments, that the product of GTP cyclohydrolase serves directly as substrate of the deaminase (*i.e.* without prior anomerization). Because it appears unlikely that GTP cyclohydrolase II would anomerize its substrate, we therefore assume that all riboside type intermediates of riboflavin biosynthesis in plants have β stereochemistry.

These data show that plants use the same pathway as eubacteria (*i.e.* via **2**) for the transformation of **1** into **4**. On the other hand, fungi use a different pathway (via **3**), and circumstantial evidence indicates that Archaea also use that pathway (50). But, to the best of our knowledge, nothing is known about the enzyme catalyzing the reduction of the ribosyl side chain in plants.

Acknowledgments—We thank Richard Feicht, Sebastian Schwamb, and Thomas Wojtulewicz for skillful help in protein preparation.

REFERENCES

1. Salomon, M., Eisenreich, W., Durr, H., Schleicher, E., Knieb, E., Massey, V., Rudiger, W., Muller, F., Bacher, A., and Richter, G. (2001) *Proc. Natl. Acad. Sci. U. S. A.* **98,** 12357–12361
2. Briggs, W. R., and Huala, E. (1999) *Annu. Rev. Cell Dev. Biol.* **15,** 33–62
3. Sancar, A. (1994) *Biochemistry* **33,** 2–9
4. Lee, J. (1985) in *Chemiluminescence and Bioluminescence* (Burr, J. G., ed) pp. 401–437, Marcel Dekker, Inc., New York
5. Lee, J., Gibson, B. G., O'Kane, D. J., Kohnle, A., and Bacher, A. (1992) *Eur. J. Biochem.* **210,** 711–719
6. Meighen, E. A. (1991) *Microbiol. Rev.* **55,** 123–142
7. Meighen, E. A. (1993) *FASEB J.* **7,** 1016–1022
8. Richter, G., Ritz, H., Katzenmeier, G., Volk, R., Kohnle, A., Lottspeich, F., Allendorf, D., and Bacher, A. (1993) *J. Bacteriol.* **175,** 4045–4051
9. Ritz, H., Schramek, N., Bracher, A., Herz, S., Eisenreich, W., Richter, G., and Bacher, A. (2001) *J. Biol. Chem.* **276,** 22273–22277
10. Kaiser, J., Schramek, N., Eberhardt, S., Püttmer, S., Schuster, M., and Bacher, A. (2002) *Eur. J. Biochem.* **269,** 5264–5270
11. Richter, G., Fischer, M., Krieger, C., Eberhardt, S., Lüttgen, H., Gerstenschläger, I., and Bacher, A. (1997) *J. Bacteriol.* **179,** 2022–2028
12. Bacher, A., Richter, G., Ritz, H., Eberhardt, S., Fischer, M., and Krieger, C. (1997) *Methods Enzymol.* **280,** 382–389
13. Richter, G., Volk, R., Krieger, C., Lahm, H. W., Röthlisberger, U., and Bacher, A. (1992) *J. Bacteriol.* **174,** 4050–4056
14. Richter, G., Krieger, C., Volk, R., Kis, K., Ritz, H., Götze, E., and Bacher, A. (1997) *Methods Enzymol.* **280,** 374–382
15. Fischer, M., Römisch, W., Schiffmann, S., Kelly, M., Oschkinat, H., Steinbacher, S., Huber, R., Eisenreich, W., Richter, G., and Bacher, A. (2002) *J. Biol. Chem.* **277,** 41410–41416
16. Steinbacher, S., Schiffmann, S., Richter, G., Huber, R., Bacher, A., and Fischer, M. (2003) *J. Biol. Chem.* **278,** 42256–42265
17. Fischer, M., Haase, I., Kis, K., Meining, W., Ladenstein, R., Cushman, M., Schramek, N., Huber, R., and Bacher, A. (2003) *J. Mol. Biol.* **326,** 783–793
18. Fischer, M., Haase, I., Feicht, R., Richter, G., Gerhardt, S., Changeux, J. P., Huber, R., and Bacher, A. (2002) *Eur. J. Biochem.* **269,** 519–526
19. Bacher, A., Eberhardt, S., Fischer, M., Mörtl, S., Kis, K., Kugelbrey, K., Scheuring, J., and Schott, K. (1997) *Methods Enzymol.* **280,** 389–399
20. Haase, I., Mörtl, S., Köhler, P., Bacher, A., and Fischer, M. (2003) *Eur. J. Biochem.* **270,** 1025–1032
21. Haase, I., Fischer, M., Bacher, A., and Schramek, N. (2003) *J. Biol. Chem.* **278,** 37909–37915
22. Schramek, N., Haase, I., Fischer, M., and Bacher, A. (2003) *J. Am. Chem. Soc.* **125,** 4460–4466
23. Zhang, X., Meining, W., Fischer, M., Bacher, A., and Ladenstein, R. (2001) *J. Mol. Biol.* **306,** 1099–1114
24. Zhang, X., Meining, W., Cushman, M., Haase, I., Fischer, M., Bacher, A., and Ladenstein, R. (2003) *J. Mol. Biol.* **328,** 167–182
25. Scheuring, J., Kugelbrey, K., Weinkauf, S., Cushman, M., Bacher, A., and Fischer, M. (2001) *J. Org. Chem.* **66,** 3811–3819

26. Mörtl, S., Fischer, M., Richter, G., Tack, J., Weinkauf, S., and Bacher, A. (1996) *J. Biol. Chem.* **271,** 33201–33207
27. Meining, W., Mörtl, S., Fischer, M., Cushman, M., Bacher, A., and Ladenstein, R. (2000) *J. Mol. Biol.* **299,** 181–197
28. Illarionov, B., Eisenreich, W., and Bacher, A. (2001) *Proc. Natl. Acad. Sci. U. S. A.* **98,** 7224–7229
29. Illarionov, B., Kemter, K., Eberhardt, S., Richter, G., Cushman, M., and Bacher, A. (2001) *J. Biol. Chem.* **276,** 11524–11530
30. Eberhardt, S., Richter, G., Gimbel, W., Werner, T., and Bacher, A. (1996) *Eur. J. Biochem.* **242,** 712–719
31. Gerhardt, S., Schott, A. K., Kairies, N., Cushman, M., Illarionov, B., Eisenreich, W., Bacher, A., Huber, R., Steinbacher, S., and Fischer, M. (2002) *Structure* (*Lond.*) **10,** 1371–1381
32. Illarionov, B., Haase, I., Bacher, A., Fischer, M., and Schramek, N. (2003) *J. Biol. Chem.* **278,** 47700–47706
33. Herz, S., Eberhardt, S., and Bacher, A. (2000) *Phytochemistry* **53,** 723–731
34. Herz, S., Kis, K., Bacher, A., and Rohdich, F. (2002) *Phytochemistry* **60,** 3–11
35. Persson, K., Schneider, G., Douglas, B. J., Viitanen, P. V., and Sandalova, T. (1999) *Protein Sci.* **8,** 2355–2365
36. Mitsuda, H., Kawai, F., Suzuki, Y., and Yoshimoto, S. (1970) *J. Vitaminol.* (*Kyoto*) **16,** 285–292
37. Bacher, A., and Eberhardt, S. (May 17, 2001) German Patent WO 2000-EP11145
38. Read, S. M., and Northcote, D. H. (1981) *Anal. Biochem.* **116,** 53–64
39. Bullock, W. O., Fernandez, J. M., and Short, J. M. (1987) *BioTechniques* **5,** 376–379
40. Stüber, D., Matile, H., and Garotta, G. (1990) in *Immunological Methods* (Lefkovits, I., and Pernis, P., eds) Vol. 4, pp. 121–152, Academic Press, Orlando, FL
41. Fischer, M., Corringer, P. J., Schott, K., Bacher, A., and Changeux, J. P. (2001) *Proc. Natl. Acad. Sci. U. S. A.* **98,** 3567–3570
42. Sanger, F., Nicklen, S., and Coulson, A. R. (1977) *Proc. Natl. Acad. Sci. U. S. A.* **74,** 5463–5467
43. Laemmli, U. K. (1970) *Nature* **227,** 680–685
44. Mann, M., and Wilm, M. (1995) *Trends Biochem. Sci.* **20,** 219–224
45. Altschul, S. F., and Koonin, E. V. (1998) *Trends Biochem. Sci.* **23,** 444–447
46. Mayer, K., Schuller, C., Wambutt, R., Murphy, G., Volckaert, G., Pohl, T., Dusterhoft, A., Stiekema, W., Entian, K. D., Terryn, N., Harris, B., Ansorge, W., Brandt, P., Grivell, L., Rieger, M., Weichselgartner, M., de Simone, V., Obermaier, B., Mache, R., Muller, M., Kreis, M., Delseny, M., Puigdomenech, P., Watson, M., and McCombie, W. R. (1999) *Nature* **402,** 769–777
47. Emanuelsson, O., Nielsen, H., Brunak, S., and von Heijne, G. (2000) *J. Mol. Biol.* **300,** 1005–1016
48. Emanuelsson, O., Nielsen, H., and von Heijne, G. (1999) *Protein Sci.* **8,** 978–984
49. Jordan, D. B., Bacot, K. O., Carlson, T. J., Kessel, M., and Viitanen, P. V. (1999) *J. Biol. Chem.* **274,** 22114–22121
50. Graupner, M., Xu, H., and White, R. H. (2002) *J. Bacteriol.* **184,** 1952–1957
51. Ireton, G. C., Black, M. E., and Stoddard, B. L. (2003) *Structure* (*Lond.*) **11,** 961–972
52. Shavlovskii, G. M., Logvinenko, E. M., Sibirnyi, A. A., Fedorovich, D. V., and Zakal'skii, A. E. (1981) *Mikrobiologiia* **50,** 1008–1011
53. Hollander, I., and Brown, G.M. (1979) *Biochem. Biophys. Res. Commun.* **89,** 759–763
54. Bacher, A., and Lingens, F. (1970) *J. Biol. Chem.* **245,** 4647–4652
55. Bacher, A., and Lingens, F. (1971) *J. Biol. Chem.* **246,** 7018–7022
56. Lingens, F., Oltmanns, O., and Bacher, A. (1967) *Z. Naturforsch.* **22,** 755–758
57. Oltmanns, O., and Bacher, A. (1972) *J. Bacteriol.* **110,** 818–822
58. Logvinenko, E. M., Stasiv Iu, Z., Zlochevskii, M. L., Voronovskii, A. I., Beburov, M. I., and Shavlovskii, G. M. (1993) *Genetika* **29,** 922–927
59. Revuelta, D. J. L., Santos, G. M. A., and Buitrago, S. M. J. (October 5, 1995) BASF A.-G., German Patent DE 94-4420785
60. Revuelta, D. J. L., Sanios, G. M. A., Garcia, R. J. J., Gonzales-Hernandez, G. A., and Buitrago, S. M. J. (May 26, 1994) BASF A.-G., German Patent DE 92-4238904
61. Zamenhof, P., and Villarejo, M. (1972) *J. Bacteriol.* **110,** 171–178